Fast Fluid Dynamics Simulation of the Airflow Around a Single Bluff Body

Huang Jiejie[1], *Ruibin* Li[1], *Zhanpeng* Liu[1], *Yi* Zhao[1], *Lu* Feng[1], *Yan* Wu[1], and *Naiping* Gao[1*]

[1]School of Mechanical Engineering, Tongji University, Shanghai, 201804, China

Abstract. Fast and accurate simulation of the outdoor airflow distribution is important for studying urban microclimate. In this paper, two pressure-correction schemes (i.e., NIPC and NSPF) for solving the N-S equation item by item are implemented in OpenFOAM and their differences from the PISO algorithm in simulating the airflow around a single 1:1:2 bluff body are analyzed. The RNG k-ε turbulence model is chosen to study the airflow disturbance, while the second-order discretization scheme of Gauss limitedLinear is used to solve the advection term in the N-S equation. The results show that the NIPC can accurately predict the main airflow characteristics around the bluff body, while the NSPF cannot predict the recirculation region on its top. The two pressure-correction schemes underestimate the TKE distribution on the top and leeward sides of the bluff body when applying the RNG k-ε turbulence model, and the maximum relative error is about 30%. However, they are consistent with the results of the PISO algorithm under the same conditions. The two schemes are about 2.5-3.0 times faster than the PSIO algorithm when run on a CPU, and the NSPF is about 12% faster than the NIPC scheme.

1 Introduction

In recent years, the scale of urban residential areas has become growing due to the acceleration of urbanization, and its unreasonable spatial configuration seriously affects the physical and mental health of residents and the comfort of their living environment [1]. Therefore, the quality of urban microclimate has received much attention, and the urban layouts should be quickly evaluated in the urban planning stage. Numerical simulation is one of the most effective methods. Unfortunately, the conventional CFD methods are computationally intensive and slow for unsteady problems [2], and thus cannot meet the demand for fast simulation of the urban microclimate over long-time spans.

Many studies focus on developing fast numerical simulation method, such as the FFD (Fast Fluid Dynamics) method. The FFD method based on the semi-Lagrangian (SL) scheme was first proposed by Stam [3] and has been widely used to quickly simulate the indoor and outdoor airflow distributions [4-7]. Zuo et al. [4] used the FFD to fast simulate the isothermal airflow distribution in a 2D cavity with a computational speed of about 30-50 times faster than the conventional CFD method. However, the FFD method adopted by Zuo et al. uses numerical viscosity as a substitute for turbulent viscosity [4], which cannot accurately predict the vortex region on the leeward side of the buildings when applying it to natural ventilation simulation [5]. Mortezazadeh and Wang [6] improved the accuracy of FFD method using a fourth-order scheme and combined it with LES to simulate the microclimate of a city [7]. However, the SL scheme does not guarantee the overall quantity conservation and may produce large numerical dissipation errors [6].

In this paper, two pressure-correction schemes for solving N-S equations item by item are implemented in OpenFOAM, and their differences from the PISO algorithm in simulating the airflow around a single 1:1:2 bluff body are analyzed. The RNG k-ε turbulence model is used to study the airflow disturbance, while the second-order discretization scheme of Gauss limitedLinear is chosen to solve the advection term in the N-S equation. The airflow distribution around a bluff body has many complex and unstable turbulence characteristics, such as flow separation, reattachment, and unsteady vortex shedding. It has been widely used to validate various numerical simulation methods and turbulence models [8].

2 Research methods

This section introduces two pressure-correction schemes for solving N-S equation item by item and their solution process. These schemes use different splitting methods to decompose the N-S equation. The momentum equations for incompressible viscous flow are as follows.

$$\frac{\partial U_i}{\partial t} + U_j \frac{\partial U_i}{\partial x_j} = -\frac{1}{\rho}\frac{\partial p}{\partial x_i} + \nu \frac{\partial^2 U_i}{\partial x_j \partial x_j} + \frac{F_i}{\rho} \quad (1)$$

where $i, j = 1, 2, 3$; U_i is the ith component of the velocity, m/s; p is the pressure, Pa; ρ is the density, kg/m^3; F_i is the ith component of the body forces, kg/(m^2·s^2); ν is the kinetic viscosity, m^2/s.

* Corresponding author: gaonaiping@tongji.edu.cn

2.1 Non-incremental pressure-correction (NIPC) scheme

The NIPC scheme was firstly proposed by Chorin [9] and used a two-step time advance method to split the momentum equation into two equations.

$$\frac{U_i^*-U_i^n}{\Delta t}+U_j^n\frac{\partial U_i^n}{\partial x_j}-\nu\frac{\partial^2 U_i^n}{\partial x_j\partial x_j}=\frac{F_i}{\rho} \quad (2)$$

$$\frac{U_i^{n+1}-U_i^*}{\Delta t}=-\frac{1}{\rho}\frac{\partial p}{\partial x_i} \quad (3)$$

where U_i^n and U_i^{n+1} represent the air velocity at previous and current time steps, respectively; U_i^* is the intermediate air velocity.

Eq. (2) can be solved by using Euler implicit scheme to the temporal term, an implicit scheme for diffusion term, and a semi-implicit scheme for advection term to obtain the air velocity U_i^*. The pressure term (i.e., Eq. (3)) is solved together with continuity equation by the pressure projection method to ensure mass conservation. Finally, the velocity U_i^{n+1} at the current time step can be solved through Eq. (3) and (4).

$$\frac{\partial^2 p}{\partial x_i\partial x_i}=\frac{\rho}{\Delta t}\frac{\partial U_i^*}{\partial x_i} \quad (4)$$

2.2 Navier-Stokes equations projection foam (NSPF) scheme

NSPF adopts the same splitting method as FFD method to split the N-S equations into the following three terms.

$$\frac{U_i^*-U_i^n}{\Delta t}=-U_j^n\frac{\partial U_i^n}{\partial x_j} \quad (5)$$

$$\frac{U_i^{**}-U_i^*}{\Delta t}=\nu\frac{\partial^2 U_i^{**}}{\partial x_j\partial x_j}+\frac{F_i}{\rho} \quad (6)$$

$$\frac{U_i^{n+1}-U_i^{**}}{\Delta t}=-\frac{1}{\rho}\frac{\partial p}{\partial x_i} \quad (7)$$

where U^{**} also represents the air velocity at the intermediate moment between the previous time step and the current time step. Unlike the FFD method based on the SL scheme, NSPF scheme uses a semi-implicit scheme for discretization and the Gauss-Seidel approach as a smoother for iterative solution. The solution process for other terms is the same as the NIPC scheme.

3 Results and analyses

3.1 Case description

The airflow around a single 1:1:2 (length (x): width (y): height (z)) bluff body is selected to verify the accuracy of the two pressure-correction schemes. The dimensions of bluff body are 0.08 m (length) × 0.08 m (width) × 0.16 m (height). The parameters of the computational domain are shown in Fig.1, and its dimensions are 25.50 H_b (x) × 13.75 H_b (y) × 11.25 H_b (z), where H_b represents the width of the bluff body. The coordinate origin is set at the center point of the bluff body. Due to space limitations, the results of the grid independence test are not shown in this paper. However, the results show that discretizing the computational domain into 189 (x) × 108 (y) × 102 (z) grid cells with the minimum grid size is about 4.44 × 10^{-3} m, which can ensure grid independence. The time step size is 0.0005 s that can maintain the stability in the solution process. For the convenience of expression, the simulation cases are named according to the numerical simulation method-turbulence model-discretization scheme in this paper. In this paper, the final normalized residual for each item is less than 1.0 × 10^{-6} as the convergence criterion. In the initial state, the velocity and pressure fields are set to zero. All cases are calculated on a personal computer (PC) with the basic configuration of "Intel(R) Core (TM) i7-10700 CPU @ 2.90GHz".

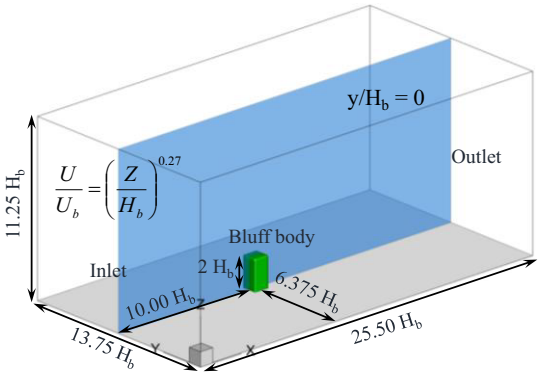

Fig. 1. Diagram of the computational domain.

The *Re* number is about 48,000 based on the height of the bluff body and inlet velocity U_b = 4.5 m/s. The power-law exponent of the vertical profile of inlet velocity is approximately 0.27. The turbulence characteristics of the inlet are calculated by the following equations.

$$k_Z=\frac{\left(\frac{kU_b}{ln((z+z_0)/z_0)}\right)^2}{\sqrt{C_\mu}} \quad (8)$$

$$\varepsilon_Z=\frac{\left(\frac{kU_b}{ln((z+z_0)/z_0)}\right)^3}{k(z+z_0)} \quad (9)$$

where κ is the von Karman constant, κ = 0.4; C_μ is a constant that takes the value of 0.9 in this paper. The ground roughness length of the computational domain is set to z_0 = 1.8 × 10^{-4} based on the experimental data [10].

3.2 Fast simulation of the airflow around a single 1:1:2 bluff body

In this section, the computational accuracy and efficiency of the two pressure-correction schemes are analyzed. The results are shown in Fig. 2. These schemes can accurately predict the main airflow characteristics around the bluff body, and the results also agree well with the experimental data, while the turbulent kinetic energy (TKE) on the top and leeward sides of the bluff body is underestimated with a maximum relative error of about 30%. However, the TKE distributions of these schemes are consistent with the results of the PISO algorithm. Therefore, this discrepancy between the simulated results and experimental data of TKE may be a common problem with the k-ε turbulence model using the isotropic eddy viscosity.

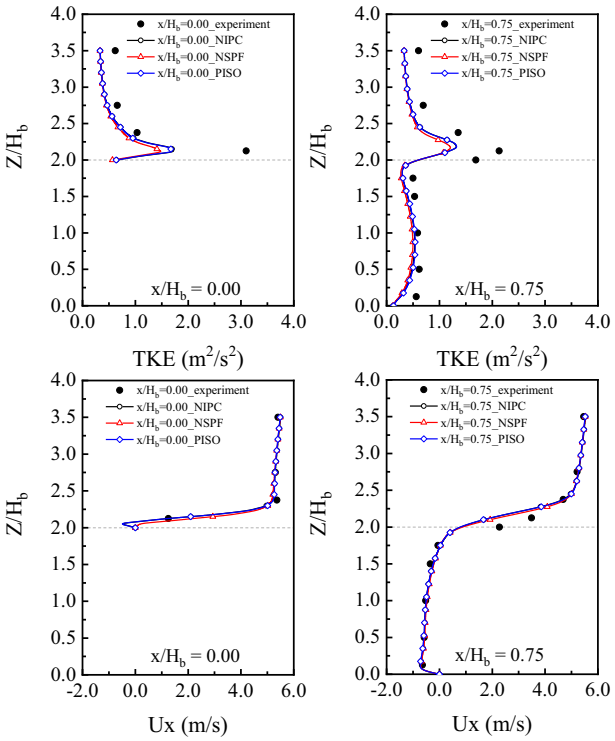

Fig. 2. Distributions of TKE and air velocity Ux on the vertical plane ($y/H_b = 0$) for different numerical simulation methods.

The results also show that there is almost no difference between the simulation results of NIPC scheme and the PISO algorithm, while the NSPF scheme cannot predict the recirculation region on the top of the bluff body, as shown in Fig. 3.

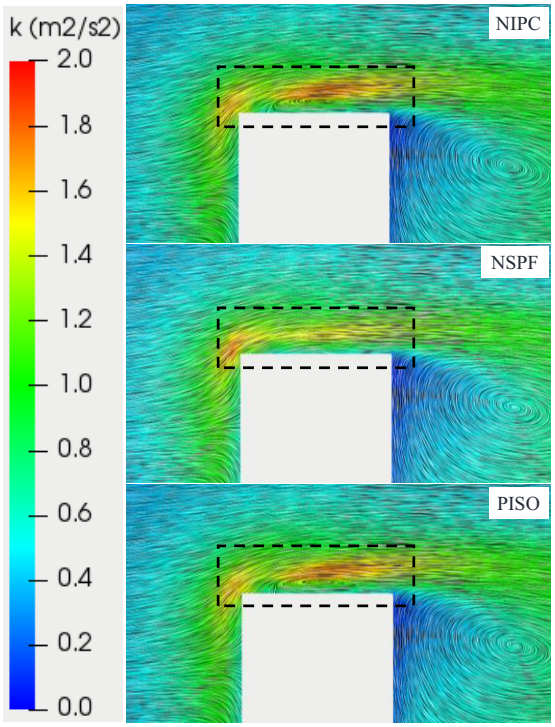

Fig. 3. Velocity vector and TKE contours on the vertical section ($y/H_b = 0$) for different numerical simulation methods.

To qualify the discrepancy, Fig. 4 shows a comparison of the percentage differences in normalized air velocity magnitude between the simulation results of the different numerical simulation methods and the experimental data. As can be seen form Fig. 4, the results of the two pressure-correction schemes applying the RNG k-ε turbulence model are acceptable for most of the locations with the relative error is less than 20% compared to the experimental data, except for the simulation results of the vortex region on the leeward side of the bluff body where there are large errors compared to experimental data. Considering the experimental data were obtained with some experimental uncertainty, which was not mentioned in more detail in the reference. Therefore, the differences between the simulation results of two pressure-correction schemes and experimental data are acceptable. These schemes can be used to quickly evaluate the different urban residential layouts in the urban planning stage.

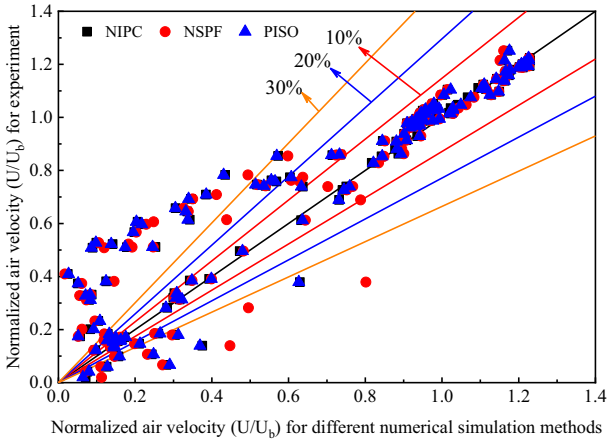

Fig. 4. Comparison of the percentage differences in normalized air velocity magnitude between the simulation results of the different numerical simulation methods and experimental data.

The dimensionless time t^* ($t^* = t_{cpu} \times U_b/H_b \times 10^{-5}$) is also used to compare the computational efficiency of the two pressure-correction schemes and the PISO algorithm, where t_{cpu} is the CPU time consumed by each simulation case. The two pressure-correction schemes are about 2.5-3.0 times faster than the PISO algorithm when applying the RNG k-ε turbulence model and second-order discretization scheme, and the NSPF is about 12% faster than the NIPC scheme. The results are shown in Table 1.

Table 1. Comparison of the computational time for different numerical simulation methods applying the RNG turbulence model and Gauss limitedLinear discretization scheme.

Numerical simulation methods	Dimensionless time t^* ($t_{cpu} \times U_b / H_b \times 10^{-5}$)
NIPC	5.506
NSPF	**4.914**
PISO	13.625

4 Discussions

In our study, the two pressure-correction schemes are about 2.5-3.0 times faster than the PISO algorithm when

applying the RNG k-ε turbulence model, but lower than the FFD method based on the SL scheme [4]. The reason for this discrepancy may be that the FFD method uses simple numerical viscosity as a substitute for turbulent viscosity and uses a simple non-slip wall treatment. We also investigated the computational speed of the two pressure-correction schemes applying the one-equation turbulence model (i.e., SpalartAllmaras, SA) and the laminar model, which are about 6.0-8.5 times faster than the PISO algorithm applying the two-equation turbulence model. Although using a simple turbulence model can improve the computational speed, its computational accuracy will be greatly affected, as shown in Fig. 5.

In addition, the configuration of a PC and the discretization schemes used to solve the advection term are also the factors that affect the computational speed. Therefore, the differences in computational accuracy and efficiency between the two pressure-correction schemes proposed in this paper and the FFD method when applied to quickly simulate the outdoor airflow distributions need to be further evaluated in detail under the same conditions.

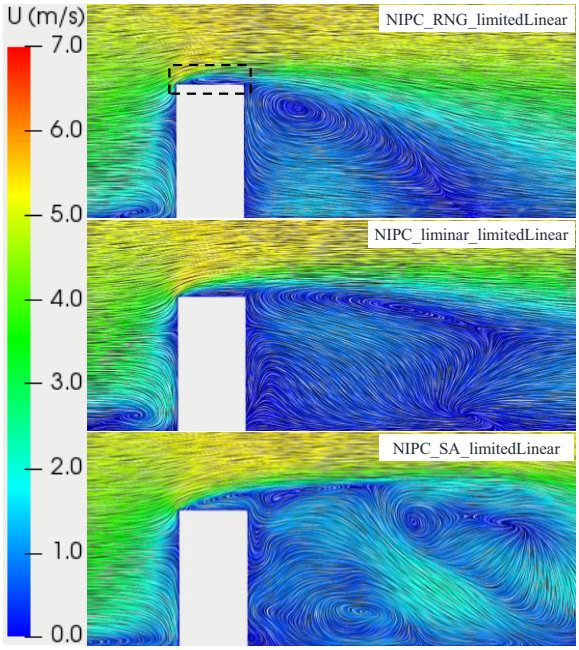

Fig. 5. Velocity vector at vertical section (y/H_b = 0) that predicted by the NIPC scheme applying the laminar and different turbulence models.

5 Conclusions

In this paper, two pressure-correction schemes are implemented in OpenFOAM and validated with the experimental data. The following conclusions are drawn.

The NIPC scheme can accurately predict the main airflow characteristics around the bluff body when applying the RNG turbulence model with a second-order discretization scheme, while the NSPF cannot predict the recirculation region on the top of the bluff body. The two pressure-correction schemes underestimate the TKE distribution on the top and leeward sides of the bluff body when applying the RNG k-ε turbulence model with a maximum relative error of about 30%. However, they are consistent with the results of the PISO algorithm. The two pressure-correction schemes are about 2.5-3.0 times faster than the PISO algorithm when applying the RNG k-ε turbulence model and second-order discretization scheme, and the NSPF is about 12% faster than the NIPC scheme. These schemes proposed in this paper can be used to quickly evaluate the different urban residential layouts in the urban planning stage.

The computational accuracy and efficiency of the two pressure-correction schemes are analyzed and validated in detail in this paper. However, the differences of two pressure-correction schemes proposed in this paper when applying different turbulence models and discretization schemes need to be further evaluated in detail, so as to find a reasonable combination scheme with certain computational accuracy and efficiency.

This work is partially supported by the National Natural Science Foundation of China under the project number of 52078353, and the Fundamental Research Funds for the Central Universities.

References

1. M. Zhen, D. Zhou, G.M. Bian, Y. Yang, Y. Liu, *Wind environment of urban residential blocks: a research review*, Archit. Sci. Rev **62**, 66-73 (2019).
2. Z. Shi, J. Chen, Q.Y. Chen, *On the turbulence models and turbulent Schmidt number in simulating stratified flows*, J. Build. Perform. Simu **9**, 134-148 (2016).
3. J. Stam, *Stable fluids*, in Proceedings of the 26th Annual Conference on Computer Graphics and Interactive Techniques, 121-128 (1999).
4. W.D. Zuo, Q.Y Chen, *Real-time or faster-than-real-time simulation of airflow in buildings*, Indoor Air **19**, 33-44 (2009).
5. M.G. Jin, W.D. Zuo, Q.Y. Chen, *Simulating natural ventilation in and around buildings by fast fluid dynamics*, Numer. Heat Tr. A-Appl **64(4)**, 273-289 (2013).
6. M. Mortezazadeh, L.Z. Wang, *A high-order backward forward sweep interpolating algorithm for semi-Lagrangian method*, Int. J. Numer. Meth. Fluids **84**, 584-597 (2017).
7. M. Mortezazadeh, L.Z. Wang, *Solving City and Building Microclimates by Fast Fluid Dynamics with Large Timesteps and Coarse Meshes*, Build. Environ **179**, 106955 (2020).
8. Y. Tominaga, A. Mochida, S. Murakami, S. Sawaki, *Comparison of various revised k-ε models and LES applied to flow around a high-rise building model with 1:1:2 shape placed within the surface boundary layer*, J. Wind Eng. Ind. Aerod **96**, 389-411 (2008).
9. A. Chorin, *Numerical solution of the Navier-Stokes equations*, Math. Comput **22(104)**, 745-762 (1968).
10. T. Meng, K. Hibi, *Turbulent measurements of the flow field around a high-rise building*, J. Wind Eng. **76**, 55-64 (1998). (In Japanese).